Female Reproductive Failures in Mouse Adolescent Pregnancy

Chen Yang
South China Agricultural University

Yue Li
South China Agricultural University

Hai-Yang Pan
South China Agricultural University

Meng-Yuan Li
South China Agricultural University

Ji-Min Pan
South China Agricultural University

Si-Ting Chen
South China Agricultural University

Hai-Yi Zhang
South China Agricultural University

Zhen-Shan Yang
South China Agricultural University

Hai-Ting Dou
South China Agricultural University

Zeng-Ming Yang (✉ zmyang@scau.edu.cn)
South China Agricultural University   https://orcid.org/0000-0001-6775-0082

Abstract

Background: There are around 300 million adolescent pregnancies worldwide, accounting for 11% of all births worldwide. Accumulating evidence demonstrates that many adverse perinatal outcomes are associated with adolescent pregnancies. However, how and why these abnormalities occur remain to be defined.

Methods: To compare uterine maturity, implantation, decidualization and placental development between 25-30 days old and 3 months old mature female CD-1 strain mice. Both in vivo mouse pregnancy and in vitro cell culture were used. Western blot, real time RT-PCR, immunostaining and immunofluorescence were used to study the progress of pregnancy during two groups.

Results: We found the litter size of adolescent pregnancy is significantly decreased from F1 to F3 generations compared to mature pregnancy. On days 8 and 12 of pregnancy, multiple abnormalities in placental and decidual developments appear in F3 adolescent pregnancy. On days 5 and 8, uterine endoplasmic reticulum stress is dysregulated compared to mature pregnancy. Embryo implantation and decidualization are also compromised in adolescent pregnancy. Many genes are abnormally expressed in adolescent estrous uteri.

Conclusion: The uterine immaturities and abnormal implantation may cause multiple pregnancy failures in adolescent pregnancy.

Introduction

Each year, about 18 million girls aged 18 years or younger become pregnant, with a higher frequency of these births by adolescents occurring in developing countries [1]. In 2015, there were about 300 million adolescent pregnancies worldwide and 16 million adolescents gave birth, accounting for 11% of all births worldwide [2]. What's more, nearly one-fifth of adolescents become pregnant in Africa [3]. In the industrialized world, the United States continues to have a high rate of adolescent pregnancy[4]. Adolescent pregnancy will still be a target for prevention in many countries[5]. Accumulating evidence demonstrates that many adverse perinatal outcomes are associated with adolescent pregnancies, such as preterm birth, low birth weight babies, preeclampsia, intrapartum death, and miscarriage[6]. Compared with women between 20 to 24.15 years old, the risk of stillbirth is 4 times higher in teens aged below 15 years and 50% higher in teens aged between 15 to 19 years [7]. In adolescents aged < 15 years, the median gestational week is lower and the rates of threatened abortion and pre-eclampsia are higher compared to control group [8]. The possibility of premature rupture of membranes and preterm premature rupture of membranes in adolescent pregnancy was significantly higher compared to adult pregnancy [9].

Because most of the perinatal complications in these newborns occurs without any chromosomal abnormality, the relationship between newborns and mothers has remained unexplained. However, most pregnancy complications associated with gestation usually have a relationship with incorrect implantation and placentation, such as preterm labor, low birth weight stillbirth and preeclampsia[10].

Embryo implantation, decidualization and placenta development are key processes during pregnancy[11]. In assisted reproductive technologies, low implantation rate is a major problem during infertility treatments [12]. Apart from embryo implantation, decidual and placental dysfunction also contribute to poor pregnancy outcomes. Impaired decidualization is closely related to preeclampsia[13]. In aged mice, there are abnormal steroid hormone responses and the decline of embryo implantation [14]. Defective decidualization and placental development also lead to abnormal embryo development and reproductive decline [10].

Based on these available data, we hypothesize that adolescent pregnancy may be associated specifically with defective decidualization and placental development. In this study, a mouse model was used to explore the factors in adolescent pregnancy leading to abnormal pregnancy outcomes. Our study showed that pregnancy outcomes are significantly compromised in adolescent pregnancy, primarily due to delayed embryo implantation and uterine immaturity.

Methods

Mice and treatments

CD1 mice were housed in a controlled environment with a 14 h light: 10 h dark cycle. Virgin females were co-caged with male CD1 mice of 8–16 weeks old. The day when vaginal plug was detected was designated as day 1 of pregnancy. The vaginal opening in CD1 virgin mice occurs about 25 days after birth, which is referenced to 14–16 years old humans [15]. To explore the effects of adolescent pregnancy on pregnancy outcomes, this study focused on immature female mice 25–30 days after birth (PND25-PND30) and mature adult mice (12 weeks). Pregnant females were designated as F0 mice, and their offspring were designated as F1 mice. F1 mice were mated at first estrus (25–30 days old), and their offspring were designated as F2 mice. F2 mice were mated at first estrus (25–30 days old), and their offspring were designated as F3 mice. Mature "Adult" females were 8–12 weeks old and designated as 3M. Artificial decidualization was performed as previously described[16]. Pregnant mice were intraperitoneally injected with Tunicamycin (TM, 0.1 or 0.001 mg/kg in saline (5 mg/ml dissolved in DMSO and diluted in saline,100 ml per mouse, Millipore) on days 6 and 7 at 9:00 and 21:00, respectively.

RT-qPCR

Total RNAs were isolated with TRIzol reagent kit (T9109, TaKaRa) and reverse transcribed with PrimeScript reverse transcriptase reagent kit (R233, Vazyme, Nanjing, China) according to the manufacturer's instructions. RT-qPCR was performed using SYBR (Q311, Vazyme, Nanjing, China) on a Bio-Rad CFX96 Touch™ Real-Time System thermocycler using gene-specific primers (Table S1). Gene expression was analyzed, and the Ct values were normalized to Rpl7 housekeeping gene.

Analysis of spliced Xbp1

Total RNAs were isolated with TRIzol reagent kit (T9109, TaKaRa) and reverse transcribed with PrimeScript reverse transcriptase reagent kit (R233, Vazyme, Nanjing, China) according to the manufacturer's instructions. *XBP1* primers were designed to contain the 26 base pair fragment for analysis of spliced and unspliced *XBP1* mRNA. Products were separated on 2.5% agarose gel. The primer sequences were described in Table S1

Isolation and culture of mouse uterine stromal cells

Stromal cells were isolated from mouse uteri. In brief, mouse uteri on day 4 of pregnancy were digested with 1% trypsin (0458, AMRESCO) and 6 mg/ml dispase (0494207801, Roche) in Hanks' balanced salt solution (H4891, Sigma). After luminal epithelial cells were removed by washing, the remaining uteri were incubated with 0.15 mg/ml collagenase I (17100017, Gibco). The isolated stromal cells were cultured in DMEM/F12 (D2906, Sigma) containing 10% charcoal-treated FBS (Biological Industries, Israel).

In vitro decidualization of endometrial stromal cells were induced with 1 mM progesterone and 10 nM 17β-estradiol as described [16].

Histology and immunohistochemistry

Tissues were fixed in 10% PBS-buffered formalin for 24 h, dehydrated and embedded in paraffin. Paraffin sections (5 μm) were deparaffinized and stained with hematoxylin and eosin for histology analysis. The number of sections of day 8 of pregnancy were collected for detected the length of embryos as previously described [17]. Immunohistochemistry was performed as previously described [18]. After blocked with 10% horse serum at 37°C for 1 h, paraffin-sections were incubated with anti-progesterone receptor (PR) (Invitrogen, MA5-A6393), anti-estrogen receptor (ER) (Santa Cruz Biotechnology, sc-7207), anti-GZMB (Abcam, ab255598), or anti-CK8 (Abcam, ab53280) overnight at 4°C. Following PBS washing, sections were incubated with biotinylated second antibody for 30 min and streptavidin-HRP complex (Zhongshan Golden Bridge) for 30 min at room temperature. The positive signals were visualized through DAB Horseradish Peroxidase Color Development Kit (Zhongshan Golden Bridge).

uNK cells were showed as previously described [19]. Briefly, paraffin-sections (5 μm) were deparaffinized and antigen-retrieved with 10 mM sodium citrate buffer (pH 6.0). After blocked with 10% horse serum at 37°C for 1 h, paraffin-sections were incubated with biotinylated dolichos biflorus agglutinin (DBA) (Sigma Aldrich, L6533) overnight at 4°C. Following PBS washing, sections were incubated with streptavidin-HRP complex (Zhongshan Golden Bridge) for 30 min at room temperature. The positive signals were visualized through DAB Horseradish Peroxidase Color Development Kit (Zhongshan Golden Bridge).

Immunofluorescence

Immunofluorescence was performed as previously described [18]. Briefly, paraffin sections were hydrated, permeabilized with 1% Triton X-100 in PBS for 10 min and blocked with 10% horse serum at 37°C for 1 h. Sections were then incubated with anti-Ki67 (ThermoFisher Scientific, RM-9106-S), anti-MUC1 (NOVUS, nb120-15481), anti-ZO-1 (Invitrogen, 61-7300), anti-Collagen 4 (Abcam, ab6586), anti-Laminin a5 (Abcam, ab184330), anti-Ezrin (Cell Signaling Technology, 3154s), anti-E-cadherin (Cell Signaling

Technology, 3195s) or anti-Lamin A (Abcam, ab26300) overnight at 4□C. After washing in PBS, sections were incubated with the corresponding second antibody conjugated with FITC for 30 min at room temperature. Sections were counter-stained with propidium iodide (PI, Sigma) and mounted for fluorescence analysis.

Western blot

Tissues or cultured cells were collected for protein extraction and protein lysates were separated by SDS polyacrylamide gel electrophoresis. After proteins were transferred onto PVDF membranes, membranes were incubated with each primary antibody overnight at 4°C. The primary antibodies used in this study included anti-GRP78 (Santa Cruz Biotechnology, sc-1050), anti-IRE (Cell Signaling Technology, 3294S), anti-p-IRE (Abcam, ab48187), anti-Tubulin (Cell Signaling Technology, 2144s)), anti-E-cadherin (Cell Signaling Technology, 3195s), anti- N-cadherin (Cell Signaling Technology, 4061s), anti-Snail (Cell Signaling Technology, 3879s), anti-cyclin D1 (Abcam, ab16663), anti-NKP46 (R&D Systems, AF2225), anti-β-actin (Cell Signaling Technology, 4967s), anti-Ezrin (Cell Signaling Technology, 3154s), anti-Lamin A (Abcam, ab26300) and anti-CHOP (Santa Cruz Biotechnology, sc-575). After membranes were incubated with the corresponding HRP-conjugated secondary antibody for 1 h, signals were detected through ECL Chemiluminescent kit (Millipore)

RNA-seq

Three samples were used for RNA-seq in 3M and F3 group. RNA-seq was performed by Novogene (Tianjing, China). Briefly, total RNAs were isolated and quantitated by Qubit® RNA Assay Kit in Qubit®2.0 Flurometer (Life Technologies, CA, USA). Total 3 μg RNAs of each sample were used for library preparation using NEBNext® UltraTM RNA Library Prep Kit for Illumina® (NEB, USA). Library preparations were sequenced with an Illumina Hiseq platform, and 125 bp/150 bp paired-end reads were generated. After raw data were first processed by in-house perl scripts, clean data were obtained by removing reads containing adapter. FPKM (Fragments per kilobase per million) of genes was calculated based on the length of genes and reads count mapped to genes. Differential expression analysis of two groups was performed by the DESeq2 R package (1.16.1). After P-values were adjusted using the Benjamini-Hochberg's approach, genes with an adjusted P-value < 0.05 were defined as differentially expressed genes. Gene Ontology (GO) enrichment analysis of differentially expressed genes was performed through the cluster Profiler R package. GO terms with corrected P value < 0.05 were considered as significantly enriched.

Statistical analysis

Data were shown by the mean ± SEM. Statistical analysis was performed with an unpaired Student's t-test or two-way ANOVA followed with Bonferroni post hoc test. At least three independent repeats were performed in all groups. $P < 0.05$ was considered statistically significant.

Results

Pregnancy outcome and placental development

After examining pregnancy outcomes for each group, we found that average litter size was significantly decreased compared 3M with F2 ($p = 0.00670$) and F3 ($p = 0.00037$) mice while no changes was showed from 3M to F1 mice ($p = 0.063648$) (Fig. 1a). Because the reduction of average litter size was obvious in F3, our further analysis focused on the comparison between F3 and 3M groups. It has been shown that decrease in litter size could result from dysfunctional uteri or decreasing embryo number [20, 21], and most problems during embryonic development are associated with placentation defects [22]. In examining day 12 (D12) pregnant mice, F3 mice were revealed to have abnormal uteri compared with 3M mice (Fig. 1b). Both the litter size and weight of embryos on D12 were decreased in F3 compared to 3M (Fig. 1c-d); there were also more abnormal embryos in F3 mice than in 3M (Fig. 1e). Therefore, we analyzed the histological structures of placentas of 3M and F3 females. Compared to 3M, the labyrinth and junctions were enlarged in the F3 group (Fig. 1f). We then examined the expression of markers of stem-like trophoblast progenitor cells differentiated from the mural trophectoderm [10, 11]. Both *Essrb* and *Eomes* were decreased in F3 abnormal conceptuses, while *Essrb* was decreased and *Eomses* was increased in F3 mice with normal embryos compared to 3M group (Fig. 2a-b). *Prl2c2* and *Tpbpa* were markers of trophoblast giant and intermediate trophoblast cells differentiated from trophoblast cells [10, 23]. Both *Prl2c2* and *Tpbpa* were decreased in F3 abnormal conceptuses, while *Prl2c2* was increased and *Tpbpa* was decreased in F3 normal conceptuses (Fig. 2c-d). *Ctsq* and *Sybn*, markers of the labyrinth layer [10], were decreased in F3 normal and abnormal conceptuses compared to the 3M group (Fig. 2e-f).

uNK cells are closely related to placental function [24]. Compared to 3M, the number of uNK cells was lower in F3 normal placenta and higher in F3 abnormal placenta (Fig. 2g). GzmB and NKP46 are essential to NK cell function. The number of GzmB-positive cells was reduced in F3 mice with normal embryos and increased in F3 mice with abnormal embryos (Fig. 2h). The mRNA expression of *GzmB* showed a similar pattern (Fig. 3a). NKP46, an NK cell-related molecule, also showed a similar change with GzmB (Fig. 3b). During placental development, NK cells are closely related to angiogenesis. *ENG* and *VEGFa*, the pro-angiogenic molecules [24], decreased in the F3 group, and Endoglin, an anti-angiogenic factor, increased (Fig. 3c-e). Decidualization genes, Prl8a2 increased while Bmp2 decreased in F3 group (Fig. 3f-g). The expression of Hoxa10 was reduced in F3 mice with normal embryos and increased in F3 mice with abnormal embryos (Fig. 3h). These data demonstrate that a dysfunctional placental may result in the decrease of litter size in the F3 group.

Decidualization during embryo development

The placenta consists of fetal and maternal cell types, which interact functionally to ensure normal embryo development. The maternal placenta is made up of the uterine decidua. Decidualization is a critical process for establishing fetal-maternal communication [25]. Because there were abnormalities for both embryonic and placental development on day 12 of pregnancy, we went further to examine decidualization and embryo development on day 8 of pregnancy. The morphological characteristics and number of embryos were similar between F3 and 3M groups (Fig. 4a-b). However, the size and weight of

the embryos decreased in the F3 group compared to the 3M group. (Fig. 4c-d). Decidual tissues from both 3M and F3 groups were chosen for transcriptome analysis. Compared to 3M, there were 337 differently expressed genes in the F3 group, of which 133 were up-regulated and 204 genes down-regulated (Fig. 4e). Among the 337 differentially expressed genes, *Igf1*, *Bmp2*, *Cdh1*, *Cited2*, Prl8a2 (*Dtprp)*, *Bmp2*, *Cited2*, *Cdh1* and *Igf1* are decidualization-related genes [10]. *Prl8a2*, *Bmp2* and *Cited2* were increased, while *Cdh1* and *Igf1* were decreased in the F3 group (Fig. 4f-j). The mesenchymal−epithelial transition (MET) is an important process during decidualization. E-cadherin, snail, and cyclin D1, MET-related genes, were decreased in the F3 group (Fig. 5a). Tight junction protein ZO-1 was significantly decreased in the F3 group (Fig. 5b). To exclude embryo effects, pseudopregnant mice were induced for artificial decidualization (Fig. 5c). The weight of deciduoma was reduced in the F3 group compared to the 3M group (Fig. 5d), and the expression of *Prl8a2* showed an increase in the F3 group (Fig. 5e). In vitro decidualization was used to examine the differences; compared to the 3M group, *Prl8a2*, *Hoxa10* and *Bmp*, decidualization-related genes, were also increased in the F3 group (Fig. 5f-h).

Dysfunction of endoplasmic reticulum stress during decidualization

The endoplasmic reticulum (ER) plays important roles in cell protein synthesis, folding, and secretion [26]. During female mammalian reproduction, proper ER stress is essential to embryo implantation and decidualization [16, 27, 28]. Based on our gene ontology (GO) and pathway analysis of differentially expressed genes on day 8 of pregnancy, genes involved in the endoplasmic reticulum chaperone complex were significantly enriched (Table S2). We then examined the protein levels of ER stress-related proteins. In the F3 group, the levels of GRP78, IRE and P-Ire were decreased compared to the 3M group, whereas CHOP levels showed no change between the two groups (Fig. 6a). In ER stress, p-IRE could splice *Xbp1* to induce gene expression [29]. On day 8 of pregnancy, the level of spliced *Xbp1* also showed a decrease in F3 groups (Fig. 6b). These data demonstrated that the dysfunction of GPR78-IRE-Xbp1 pathway could be one cause of the deregulation of decidualization in the F3 group compared to 3M.

To further examine the response of pregnant mice to ER stress, female mice were treated on day 6 and day 7 at 9:00 and 21:00 with different doses of TM (Tunicamycin), an inducer of unfolded protein response by blocking N-linked glycosylation. When 3M pregnant mice were treated with 0.001 mg/kg TM, the weight of implantation sites on D8 remained unchanged compared to control. After F3 pregnant mice were treated with 0.001 mg/kg TM, the weight of embryos significantly decreased (Fig. 6c-e). When 3M mice were treated with 0.1mg/kg TM, the weight of embryos was decreased, and both Grp78 and Ire increased compared to control. When F3 mice were treated with 0.1 mg/kg TM, embryos were obviously reabsorbed, and both Grp78 and Ire were decreased (Fig. 6c-d). These results suggest that ER stress dysfunction could be related to decidualization deregulation in F3 mice due to a differing response by uterine stromal cells.

Decreased endoplasmic reticulum during embryo implantation

In rodents, embryo implantation is the premise of decidualization. Abnormal embryo implantation is related to the dysfunction of decidualization [30]. To explore the reason for decidualization dysfunction, we examined embryo implantation on D6. We found that embryo implantation sites were similar between F3 and 3M groups (Fig. 7a-b). However, there were fewer implantation sites on day 5 in the F3 group compared to the 3M group (Fig. 7c-d). For ER stress, the mRNA levels of GRP78 and IRE were significantly decreased in F3 group. The levels of Ire and p-Ire proteins also showed an abnormal pattern in F3 group (Fig. 7e-f). Furthermore, *XBP1* expression was decreased in the F3 group due to the decreased p-IRE (Fig. 7g). These data suggest that embryo implantation and ER stress was deregulated in the F3 group.

Delayed implantation due to receptive uterus

We further examined whether embryo implantation is normal on day 4 of pregnancy. At 22:00 on day 4, a few implantation sites appeared in the 3M group, but no implantation sites were detected in the F3 group. At 24:00 of day 4, implantation sites were detected clearly in the 3M group compared with F3 group (Fig. 8a). Based on this study, we wondered whether embryonic development is normal in the morning of day 4 pregnancy. When we flushed uteri in the morning on day 4, the number of blastocysts was similar between 3M and F3 (Fig. 8b). The morphology of blastocysts was also similar between 3M and F3 groups (Fig. 8c). These results suggest that the delay of embryo implantation might be from a uterine response in the F3 group.

Estrogen is a critical factor in determining the beginning of the implantation window. Estrogen level determines the duration of the implantation window within a very narrow range. To analyze the cause of delayed implantation, we measured estrogen levels on day 4. In the F3 group, estrogen levels were significantly higher than that of the 3M group (Fig. 8d). *Ltf*, *Muc1* and *Pgr*, estrogen targeted genes, were also increased in the F3 group (Fig. 8e-g), as were immunostained levels of ER and PGR (Fig. 8h-i) and MUC1and KI67 (Fig. 9a-b), which are closely related to embryo implantation. The remodeling of the extracellular matrix is important for embryo implantation [31]. Collagen 4 and Laminin a5, key components of the extracellular matrix [32], were also increased in the F3 group. Ezrin, which is down-regulated during embryo implantation [33], was increased in F3 mice (Fig. 9c-e). These results illustrate that uteri receptivity was compromised in the F3 group compared to 3M group.

Immature uterus in F3 group

Because F3 mice were 25–30 days old, we wondered whether uteri were matured in these mice. Glands are required for embryo implantation, yet in F3 mice at estrus, the size of the uterus and the number of glands were significantly decreased (Fig. 10a). Except for glandular development, tight junction and the extracellular matrix are also important for uterine development. E-cadherin, an adherence junction protein [34], was strongly detected in the epithelial cells in 3M mice compared to F3 mice (Fig. 10b). Collagen IV, a key component of the extracellular matrix, was also strongly seen in 3M mice compared to F3 mice (Fig. 10c). Compared to 3M mice, Ezrin was highly detected on the surface of epithelial cells in F3 group (Fig. 10d, g). Lamin A, a main component of the nuclear lamina, was decreased in uterine stromal cells

and glandular epithelial cells in the F3 group compared to the 3M group (Fig. 10e-f). These data demonstrate that uteri in F3 mice are underdeveloped compared to those in 3M mice.

Discussion

Adolescent pregnancy is associated with perinatal outcomes such as preterm birth, low birth weight babies, and preeclampsia [35]. These abnormalities could be related to both embryonic and maternal factors. In this study, we found that the litter size of F3 mice is significantly decreased. Although development of preimplantation embryos was normal, the uterine immaturities of F3 mice likely triggered abnormal pregnancy outcomes.

Most pregnancy complications such as low birth weight, fetal growth restriction, and pre-eclampsia are correlated with a failure of proper placentation [36]. During pregnancy, the placenta is the main regulator of nutrient supply for the growing embryo. Adequate placental function is indispensable for developmental progression during intrauterine development [23]. A recent study indicated that sub-viable mouse mutants or embryonic lethal models are associated with labyrinthian defects and intrauterine growth retardation prior to death [37]. In our study, labyrinth markers are significantly decreased in abnormal embryos of F3 mice. Evidence from individual gene knockouts also demonstrated that placental labyrinth development is directly associated with fetal growth [38]. In the F3 group, the labyrinth shows defective development and fetal growth is retarded. Improper differentiation also occurs in stem-like trophoblast progenitor cells, the intermediate trophoblasts, spongiotrophoblast (SpTr) Tpbpa and trophoblast giant cells in the F3 group. Ablation of Tpbpa-positive cells results in trophoblast invasion defects, which are related to defective remodeling of maternal spiral arteries [39].

From days 6–11 of pregnancy in mice, uNK cells are recruited in large numbers to the mesometrial decidua[40]. uNK cells could be the key regulator of placental vascularization, including spiral artery remodeling[41]. The combination of uNK cells and maternal β3 integrin showed profound effects on invasive trophoblasts and placental development [24]. In our study, the decrease of uNK cell number and abnormal expression patterns of angiogenic cytokines suggest placental dysfunction, which could be the cause of lower litter sizes in F3 mice.

The correct development of placentation is closely related to uterine decidualization, as the decidua functions as one part of the placenta [42]. Although the number of implantation sites showed similar patterns in two groups on day 8 of pregnancy, the length and weight of embryos were significantly decreased in the F3 group. Dysfunction of decidualization is an important cause of preeclampsia [43]; in women with preeclampsia, decidual cells exhibited inadequate decidualization [44]. Through microarray data analysis, the molecular pathways of decidualization were shown to be dysregulated in preeclampsia and endometrial disorders [45]. Based on our transcriptome analysis, many pathways were significantly changed in the F3 group, including the bicellular tight junction and endoplasmic reticulum chaperone complex. Artificial decidualization is also compromised in the F3 group. The mesenchymal–epithelial transition is an important step during decidualization[46]. In F3 mice, genes involved in mesenchymal–

epithelial transition are down-regulated. During preeclampsia pregnancies, MET showed an increased pattern in the decidua [47]. In aged mice, decidualization defects cause reproductive decline, key regulators of decidualization are downregulated [10], and artificially-induced decidual response is also defective [48]. These studies suggest that proper decidualization is essential for successful pregnancy.

During early pregnancy in mice, Ire-xbp1 signaling pathway of ER stress is activated in decidual cells on days 5–8 of pregnancy [16]. GRP78 is expressed at implantation sites and decidual cells[16]. In human decidual cells, the Ire-xbp1 signaling pathway is induced to support embryo development [28]. In patients with spontaneous labor and preterm labor, GRP78, IRE1, and spliced $Xbp1$ ($sXbp1$) are significantly increased [49]. Compared to normal pregnancy, unspliced $Xbp1$ ($uXbp1$) is increased in decidual cells of preeclampsia patients [50]. Mouse decidualization is impaired after Ire-xbp1 signaling pathway is inhibited [16]. These studies suggest that ER stress is a physiological process during embryo implantation and decidualization. In our study, ER stress is decreased in the F3 group, indicating that deregulation of ER stress could be one cause of dysfunctional decidualization.

TM has a concentration- and time-dependent effect on the proliferation of stromal cells [16]. Treatment with 50 ng/ml or 2.5 µg/ml TM inhibits cell proliferation and growth[51]. However, treatment with TM at pg/ml level has the opposite effect [52]. In this study, treatment with 0.001 mg/kg TM causes a decrease of implantation sites in the F3 group but has no effects in 3M mice, and treatment with 0.1 mg/kg TM causes more severe effects in the F3 group. These results indicate the response of ER stress is more sensitive in the F3 group than in the 3M group. In aged human skeletal muscles, many key components of the unfolded protein response are decreased, resulting in dysfunctional ER stress [53]. Therefore, it is possible that the young age of F3 mice may cause abnormal ER stress.

Proper embryo implantation is required for successful establishment of pregnancy. In mice, estrogen is a key determinant for the duration of the window of uterine receptivity; specifically, a high level of estrogen will shorten the window of implantation [54]. In this study, the serum estrogen level and the expression levels of estrogen-targeted genes are significantly higher in the F3 group than in the 3M group. A previous study demonstrated that estrogen levels are also upregulated in Rbpj$^{d/d}$ female mice, leading to abnormal decidualization and embryonic lethality [30]. In aged mice, the estrogen-responsive genes are downregulated [10, 14]. The decrease of uterine estrogen response may contribute to the decline of pregnancy rate [14]. It is possible that the increase of both estrogen and uterine estrogen response may result in the decline of pregnancy in the F3 group.

Adequate uterine development is a requirement for pregnancy establishment. Uterine glands are necessary for uterine function. In the glandless uterus of FOXA2-deficient mice, embryo resorption and pregnancy failure occur [55]. Glands are fundamental to pregnancy success, as they directly connect the crypt encasing the embryo [56]. In our study, the number of glands is significantly decreased in F3 mice. Collagens and Lamins of extracellular matrix components are upregulated in human receptive endometrium[57]. Collagens are important for embryo implantation [58]. Lamins are key structural components of the nuclear lamina and play a role in nuclear architecture, DNA replication, and gene

expression [59]. In the F3 group, both collagen IV and lamin A in stromal cells are downregulated, indicating that the extracellular matrix and stromal cells may be immature. Cadherins are adhesion molecules expressed at the cellular membrane for controlling cell adhesion [60]. Ezrin is one ERM protein that provides a critical link between the plasma membrane and surface structures and is present in uterine epithelium in human endometrial cycle and downregulated during embryo implantation[33]. In F3 mice, upregulated Ezrin and downregulated E-cadherin indicated tight junction in epithelial cells was not well developed.

Conclusions

In summary, this study extensively compares different stages of adolescent and normal pregnancy. We found numerous abnormalities during adolescent pregnancy, including decidual and placental defects and small litter size. These abnormalities may result from uterine immaturity, high levels of estrogen and abnormal response of ER stress. As a result, this study sheds light on adolescent pregnancy and the underlying factors that lead to adverse perinatal outcomes, including preterm birth, low birth weight babies, preeclampsia, intrapartum death, and miscarriage, which substantially affect maternal and neonatal health.

List Of Abbreviations

E2: Estradiol-17β; DMSO: Dimethyl sulfoxide; ER stress: Endoplasmic reticulum stress; MET: Mesenchymal−epithelial transition; TM: Tunicamycin; uNK cell: Uterine nature kill cell; GO: Gene Ontology

Declarations

Ethics approval and consent to participate
All animal experiments were approved by the Animal Use and Care Committee of South China Agricultural University.

Consent for publication
Not applicable

Competing interests

The authors declare that they have no competing interests.

Funding

Authors' contributions

CY and ZMY designed this study and wrote the paper. YL, HYZ, MYL, ZSY conducted mouse work, RT-PCR and Western blots. JMP, HYP and STC performed immunofluorescence experiments. CY and ZSY performed RNA sequencing analyses and analyzed data.

Availability of data and materials

Raw data from RNA sequencing of decidua on days 8 of pregnancy have been deposited in GEO under the accession code SUB9120346. All data of this study are available from the corresponding author on reasonable request.

References

1. Monteiro DLM, Martins J, Rodrigues NCP, Miranda FRD, Lacerda IMS, Souza FM, Wong ACT, Raupp RM, Trajano AJB: **Adolescent pregnancy trends in the last decade.***Rev Assoc Med Bras (1992)* 2019, **65**:1209–1215.

2. Holness N: **A global perspective on adolescent pregnancy.***Int J Nurs Pract* 2015, **21**:677–681.

3. Kassa GM, Arowojolu AO, Odukogbe AA, Yalew AW: **Prevalence and determinants of adolescent pregnancy in Africa: a systematic review and Meta-analysis.***Reproductive Health* 2018, **15**.

4. Jiskrova GK, Vazsonyi AT: **Multi-contextual influences on adolescent pregnancy and sexually transmitted infections in the United States.***Soc Sci Med* 2019, **224**:28–36.

5. Marvin-Dowle K, Soltani H: **A comparison of neonatal outcomes between adolescent and adult mothers in developed countries: A systematic review and meta-analysis.***Eur J Obstet Gynecol Reprod Biol X* 2020, **6**:100109.

6. Leftwich HK, Alves MV: **Adolescent Pregnancy.***Pediatr Clin North Am* 2017, **64**:381–388.

7. Kramer KL, Lancaster JB: **Teen motherhood in cross-cultural perspective.***Ann Hum Biol* 2010, **37**:613–628.

8. Karata V, Kanmaz AG, Inan AH, Budak A, Beyan E: **Maternal and neonatal outcomes of adolescent pregnancy.***Journal of Gynecology Obstetrics and Human Reproduction* 2019, **48**:347–350.

9. Markovic S, Bogdanovic G, Cerovac A: **Premature and preterm premature rupture of membranes in adolescent compared to adult pregnancy.***Med Glas (Zenica)* 2020, **17**:136–140.

10. Woods L, Perez-Garcia V, Kieckbusch J, Wang XQ, DeMayo F, Colucci F, Hemberger M: **Decidualisation and placentation defects are a major cause of age-related reproductive decline.***Nature Communications* 2017, **8**.

11. Hemberger M, Hanna CW, Dean W: **Mechanisms of early placental development in mouse and humans.***Nature Reviews Genetics* 2020, **21**:27–43.

12. Dey SK, Lim H, Das SK, Reese J, Paria BC, Daikoku T, Wang HB: **Molecular cues to implantation.***Endocr Rev* 2004, **25**:341–373.

13. Zhou Q, Yan G, Ding L, Liu J, Yu X, Kong S, Zhang M, Wang Z, Liu Y, Jiang Y, et al: **EHD1 impairs decidualization by regulating the Wnt4/beta-catenin signaling pathway in recurrent implantation failure.***EBioMedicine* 2019, **50**:343–354.

14. Li MQ, Yao MN, Yan JQ, Li ZL, Gu XW, Lin S, Hu W, Yang ZM: **The decline of pregnancy rate and abnormal uterine responsiveness of steroid hormones in aging mice.***Reprod Biol* 2017, **17**:305–311.

15. Wu S, Divall S, Hoffman GE, Le WW, Wagner KU, Wolfe A: **Jak2 is necessary for neuroendocrine control of female reproduction.***J Neurosci* 2011, **31**:184–192.

16. Gu XW, Yan JQ, Dou HT, Liu J, Liu L, Zhao ML, Liang XH, Yang ZM: **Endoplasmic reticulum stress in mouse decidua during early pregnancy.***Mol Cell Endocrinol* 2016, **434**:48–56.

17. Li SJ, Wang TS, Qin FN, Huang Z, Liang XH, Gao F, Song Z, Yang ZM: **Differential regulation of receptivity in two uterine horns of a recipient mouse following asynchronous embryo transfer.***Sci Rep* 2015, **5**.

18. Hu W, Liang YX, Luo JM, Gu XW, Chen ZC, Fu T, Zhu YY, Lin S, Diao HL, Jia B, Yang ZM: **Nucleolar stress regulation of endometrial receptivity in mouse models and human cell lines.***Cell Death Dis* 2019, **10**.

19. Chen ZL, Zhang JH, Hatta K, Lima PDA, Yadi H, Colucci F, Yamada AT, Croy BA: **DBA-Lectin reactivity defines mouse uterine natural killer cell subsets with biased gene expression.***Biol Reprod* 2012, **87**.

20. Ye X, Hama K, Contos JJ, Anliker B, Inoue A, Skinner MK, Suzuki H, Amano T, Kennedy G, Arai H, et al: **LPA3-mediated lysophosphatidic acid signalling in embryo implantation and spacing.***Nature* 2005, **435**:104–108.

21. Kim BH, Ju WS, Kim JS, Kim SU, Park SJ, Ward SM, Lyu JH, Choo YK: **Effects of gangliosides on spermatozoa, oocytes, and preimplantation embryos.***Int J Mol Sci* 2019, **21**.

22. Copp AJ: **Death before birth: clues from gene knockouts and mutations.***Trends Genet* 1995, **11**:87–93.

23. Woods L, Perez-Garcia V, Hemberger M: **Regulation of placental development and its impact on fetal growth-new insights from mouse models.***Front Endocrinol (Lausanne)* 2018, **9**.

24. Yougbare I, Tai WS, Zdravic D, Oswald BE, Lang S, Zhu GH, Leong-Poi H, Qu DW, Yu LS, Dunk C, et al: **Activated NK cells cause placental dysfunction and miscarriages in fetal alloimmune thrombocytopenia.***Nature Communications* 2017, **8**.

25. Gellersen B, Brosens JJ: **Cyclic decidualization of the human endometrium in reproductive health and failure.***Endocr Rev* 2014, **35**:851–905.

26. Ron D, Walter P: **Signal integration in the endoplasmic reticulum unfolded protein response.***Nature Reviews Molecular Cell Biology* 2007, **8**:519–529.

27. Lin PF, Jin YP, Lan XL, Yang YZ, Chen FL, Wang N, Li X, Sun YJ, Wang AH: **GRP78 expression and regulation in the mouse uterus during embryo implantation.***Journal of Molecular Histology* 2014, **45**:259–268.

28. Brosens JJ, Salker MS, Teklenburg G, Nautiyal J, Salter S, Lucas ES, Steel JH, Christian M, Chan YW, Boomsma CM, et al: **Uterine Selection of Human Embryos at Implantation.***Sci Rep* 2014, **4**.

29. Calfon M, Zeng HQ, Urano F, Till JH, Hubbard SR, Harding HP, Clark SG, Ron D: **IRE1 couples endoplasmic reticulum load to secretory capacity by processing the XBP-1 mRNA (vol 415, pg 92, 2002).***Nature* 2002, **420**:202–202.

30. Zhang S, Kong SB, Wang BY, Cheng XH, Chen YJ, Wu WW, Wang Q, Shi JC, Zhang Y, Wang SM, et al: **Uterine Rbpj is required for embryonic-uterine orientation and decidual remodeling via Notch pathway-independent and -dependent mechanisms.***Cell Res* 2014, **24**:925–942.

31. Ye XQ: **Uterine luminal epithelium as the transient gateway for embryo implantation.***Trends Endocrinol Metab* 2020, **31**:165–180.

32. Lecce L, Lindsay LA, Murphy CR: **Ezrin and EBP50 redistribute apically in rat uterine epithelial cells at the time of implantation and in response to cell contact.***Cell Tissue Res* 2011, **343**:445–453.

33. Haeger JD, Hambruch N, Dantzer V, Hoelker M, Schellander K, Klisch K, Pfarrer C: **Changes in endometrial ezrin and cytokeratin 18 expression during bovine implantation and in caruncular endometrial spheroids in vitro.***Placenta* 2015, **36**:821–831.

34. Lee B, Moon KM, Kim CY: **Tight junction in the intestinal epithelium: Its association with diseases and regulation by phytochemicals.***Journal of Immunology Research* 2018, **2018**.

35. Brosens I, Benagiano G, Brosens JJ: **The potential perinatal origin of placentation disorders in the young primigravida.***Am J Obstet Gynecol* 2015, **212**:580–585.

36. Norwitz ER: **Defective implantation and placentation: laying the blueprint for pregnancy complications.***Reproductive Biomedicine Online* 2006, **13**:591–599.

37. Perez-Garcia V, Fineberg E, Wilson R, Murray A, Mazzeo CI, Tudor C, Sienerth A, White JK, Tuck E, Ryder EJ, et al: **Placentation defects are highly prevalent in embryonic lethal mouse mutants.***Nature* 2018, **555**:463-+.

38. Watson ED, Cross JC: **Development of structures and transport functions in the mouse placenta.***Physiology (Bethesda)* 2005, **20**:180–193.

39. Hu D, Cross JC: **Ablation of Tpbpa-positive trophoblast precursors leads to defects in maternal spiral artery remodeling in the mouse placenta.***Dev Biol* 2011, **358**:231–239.

40. Kieckbusch J, Gaynor LM, Moffett A, Colucci F: **MHC-dependent inhibition of uterine NK cells impedes fetal growth and decidual vascular remodeling (vol 5, 3359, 2014).***Nature Communications* 2017, **8**.

41. Wallace AE, Whitley GS, Thilaganathan B, Cartwright JE: **Decidual natural killer cell receptor expression is altered in pregnancies with impaired vascular remodeling and a higher risk of pre-eclampsia.***J Leukoc Biol* 2015, **97**:79–86.

42. Ramathal CY, Bagchi IC, Taylor RN, Bagchi MK: **Endometrial decidualization: Of mice and men.***Semin Reprod Med* 2010, **28**:17–26.

43. Garrido-Gomez T, Dominguez F, Quinonero A, Diaz-Gimeno P, Kapidzic M, Gormley M, Ona K, Padilla-Iserte P, McMaster M, Genbacev O, et al: **Defective decidualization during and after severe preeclampsia reveals a possible maternal contribution to the etiology.***Proc Natl Acad Sci U S A* 2017, **114**:E8468-E8477.

44. Sahu MB, Deepak V, Gonzales SK, Rimawi B, Watkins KK, Smith AK, Badell ML, Sidell N, Rajakumar A: **Decidual cells from women with preeclampsia exhibit inadequate decidualization and reduced sFlt1 suppression.***Pregnancy Hypertension-an International Journal of Womens Cardiovascular Health* 2019, **15**:64–71.

45. Rabaglino MB, Conrad KP: **Evidence for shared molecular pathways of dysregulated decidualization in preeclampsia and endometrial disorders revealed by microarray data integration.***FASEB J* 2019, **33**:11682–11695.

46. Zhang XH, Liang X, Liang XH, Wang TS, Qi QR, Deng WB, Sha AG, Yang ZM: **The Mesenchymal-Epithelial Transition During In Vitro Decidualization.***Reprod Sci* 2013, **20**:354–360.

47. Chen JS, Ren WL, Lin L, Zeng SS, Huang LJ, Tang JM, Bi SL, Pan JH, Chen DJ, Du LL: **Abnormal cGMP-dependent protein kinase I-mediated decidualization in preeclampsia.***Hypertens Res* 2020.

48. Finch CE, Holinka CF: **Aging and uterine growth during implantation in C57BL/6J mice.***Exp Gerontol* 1982, **17**:235–241.

49. Liong S, Lappas M: **Endoplasmic Reticulum Stress Is Increased after Spontaneous Labor in Human Fetal Membranes and Myometrium Where It Regulates the Expression of Prolabor Mediators.***Biol Reprod* 2014, **91**.

50. Lian IA, Loset M, Mundal SB, Fenstad MH, Johnson MP, Eide IP, Bjorge L, Freed KA, Moses EK, Austgulen R: **Increased endoplasmic reticulum stress in decidual tissue from pregnancies complicated by fetal growth restriction with and with out pre-eclampsia.***Placenta* 2011, **32**:823–829.

51. Shen MZ, Wang L, Quo MW, Xue Q, Hu C, Li X, Fan L, Wang XM: **A novel endoplasmic reticulum stress-induced apoptosis model using tunicamycin in primary cultured neonatal rat cardiomyocytes.***Mol Med Report* 2015, **12**:5149–5154.

52. Jin C, Jin Z, Chen NZ, Lu M, Liu CB, Hu WL, Zheng CG: **Activation of IRE1 alpha-XBP1 pathway induces cell proliferation and invasion in colorectal carcinoma.***Biochem Biophys Res Commun* 2016, **470**:75–81.

53. Deldicque L: **Endoplasmic reticulum stress in human skeletal muscle: any contribution to sarcopenia?** *Front Physiol* 2013, **4**.

54. Ma WG, Song H, Das SK, Paria BC, Dey SK: **Estrogen is a critical determinant that specifies the duration of the window of uterine receptivity for implantation.***Proc Natl Acad Sci U S A* 2003, **100**:2963–2968.

55. Kelleher AM, Milano-Foster J, Behura SK, Spencer TE: **Uterine glands coordinate on-time embryo implantation and impact endometrial decidualization for pregnancy success.***Nature Communications* 2018, **9**.

56. Yuan JB, Deng W, Cha J, Sun XF, Borg JP, Dey SK: **Tridimensional visualization reveals direct communication between the embryo and glands critical for implantation.***Nature Communications* 2018, **9**.

57. Haller-Kikkatalo K, Altmae S, Tagoma A, Uibo R, Salumets A: **Autoimmune Activation toward Embryo Implantation is Rare in Immune-Privileged Human Endometrium.***Semin Reprod Med* 2014, **32**:376–384.

58. Zheng HT, Zhang HY, Chen ST, Li MY, Fu T, Yang ZM: **The detrimental effects of stress-induced glucocorticoid exposure on mouse uterine receptivity and decidualization.***FASEB J* 2020, **34**:14200–14216.

59. Vergnes L, Peterfy M, Bergo MO, Young SG, Reue K: **Lamin B1 is required for mouse development and nuclear integrity.***Proc Natl Acad Sci U S A* 2004, **101**:10428–10433.

60. Achache H, Revel A: **Endometrial receptivity markers, the journey to successful embryo implantation.**_Hum Reprod Update_ 2006, **12**:731–746.
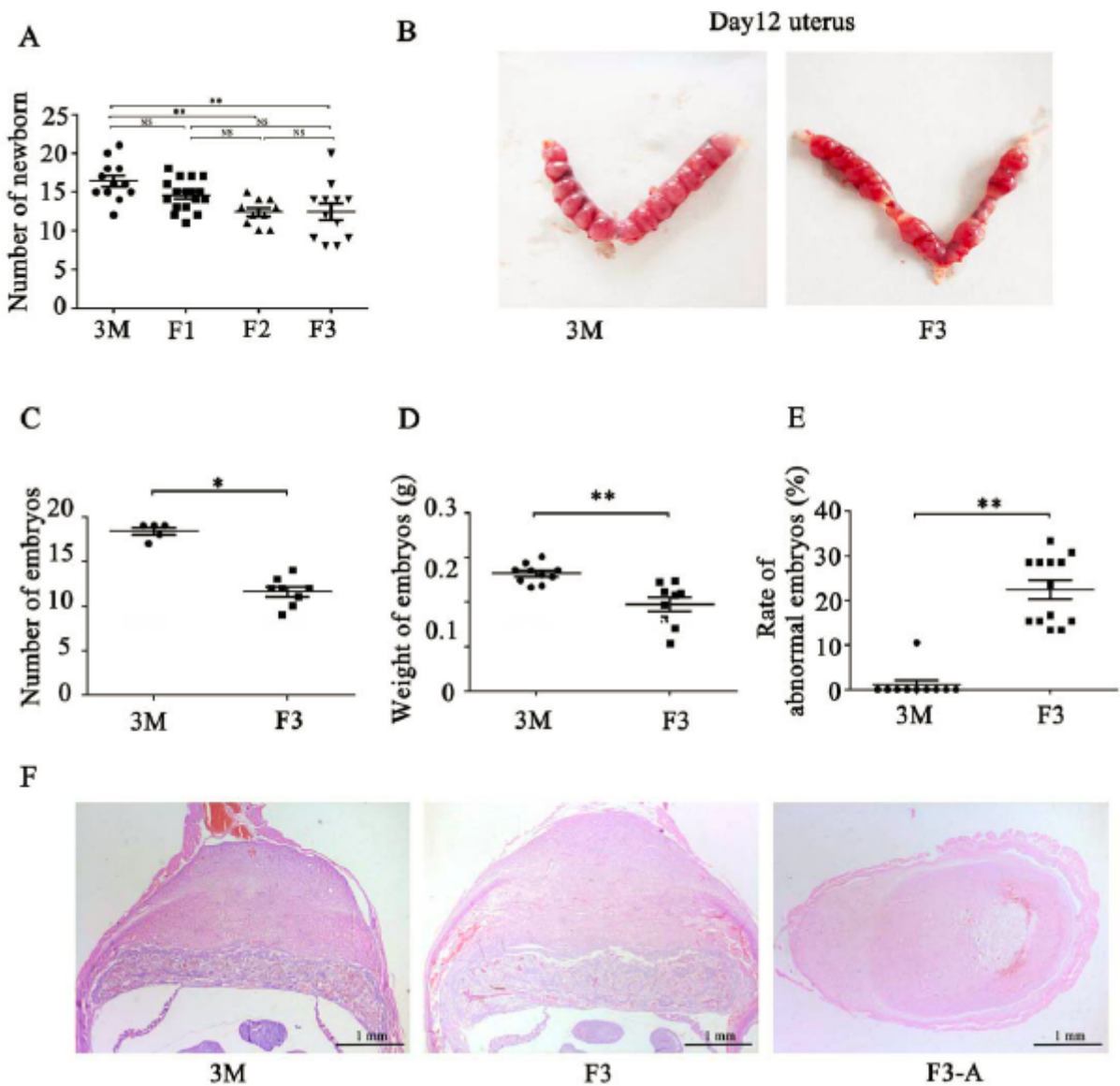
Figures

Figure 1

Pregnancy outcomes and placental development. (a) The average number of newborn mice in 3M (Adult group, n =12), F1 (Adolescent F1, n =17), F2 (Adolescent F2, n =10), and F3 (Adolescent F3, n =12). Statistical differences are analyzed by ANOVA followed by Tukey's multiple comparisons post-hoc test. Data are present as mean ± S.E.M. **p < 0.01. (b) The uterine morphology on day 12 of pregnancy. (c) The average number of embryos on day 12. (d) The average weight of embryos on day 12. (e) The rate of abnormal embryos (n=12). (f) The placental morphology on day 12. Scale bars: 1 mm, n =6
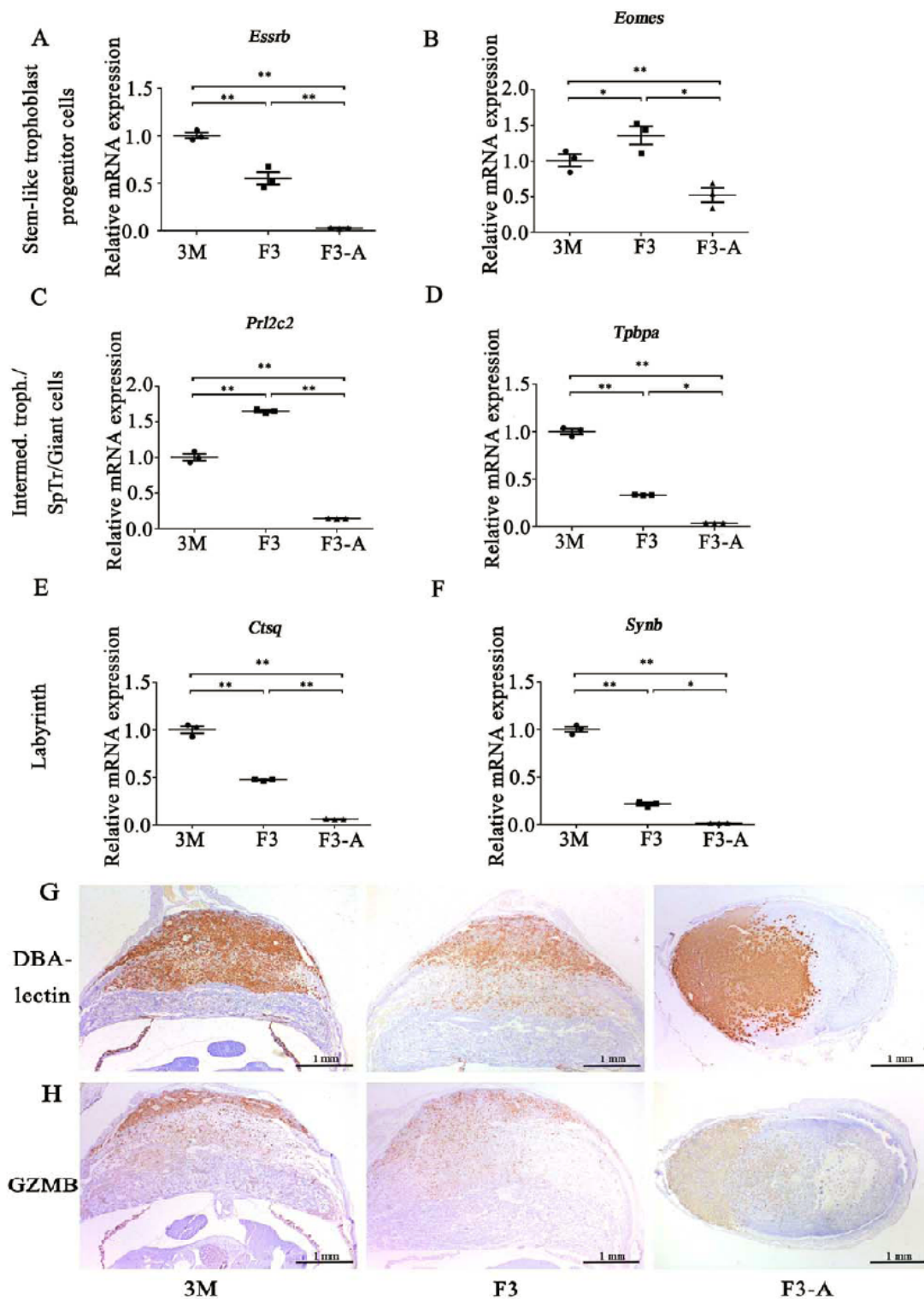
Figure 2

Placental development and uNK cells on day 12 of pregnancy in 3M (n = 6), normal F3 (n= 6) and abnormal F3 (F3-A, n= 6) groups. (a, b) The mRNA levels of Essrb and Eomes, markers of trophoblast stem cell genes. (c, d) The mRNA levels of Prl2c2 and Tpbpa, markers of the intermediate trophoblast giant cells. (e, f) The mRNA level of Ctsq and Synb, markers of placental labyrinths. (g) The distribution of

uNK cells. (h) GzmB immunostaining. Scale bars: 1 mm. Statistical differences are analyzed by ANOVA followed by Tukey's multiple comparisons post-hoc test. Data are present as mean ± S.E.M. **p < 0.01.
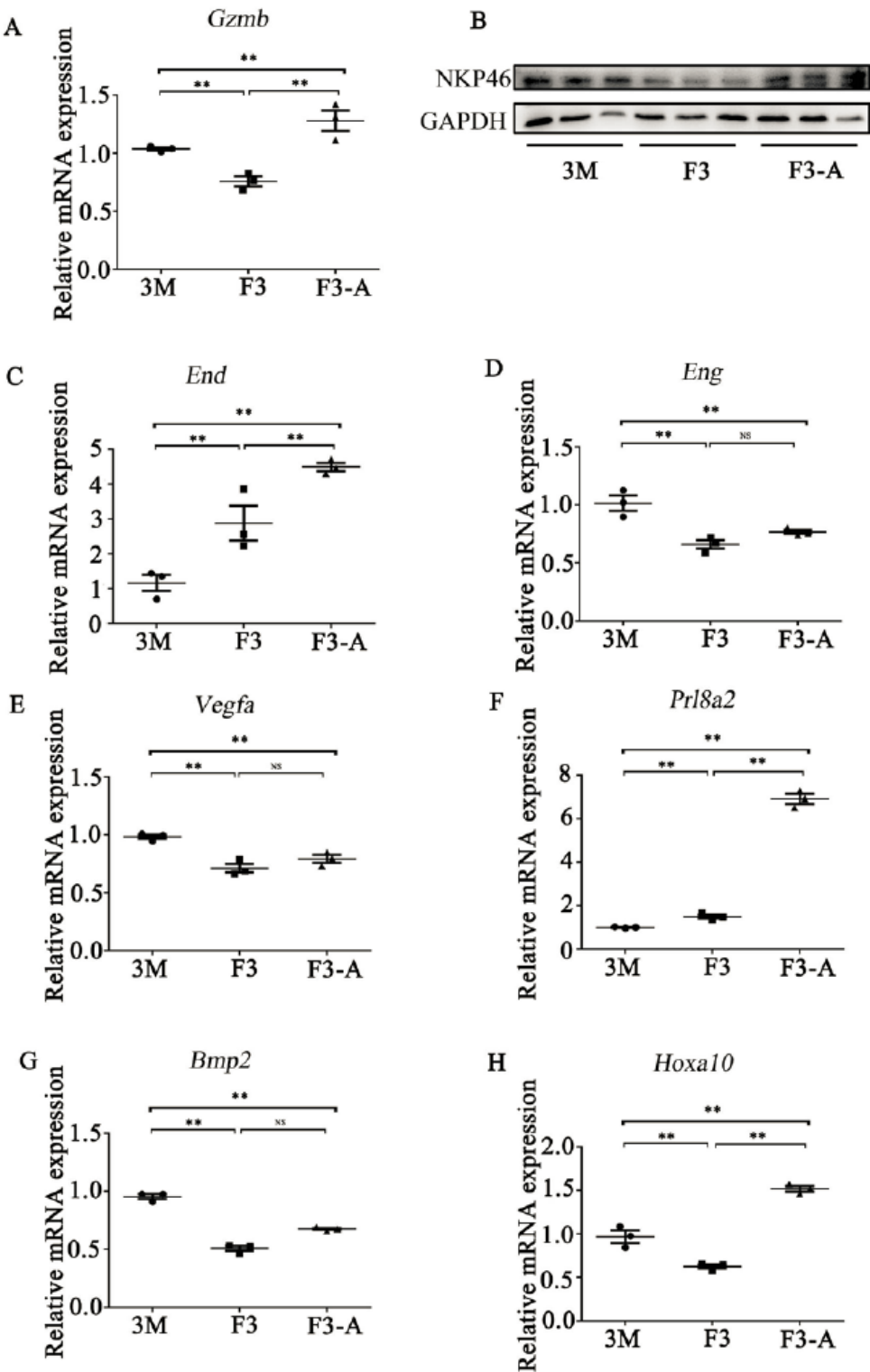
Figure 3

Decidualization changes in placenta on day 12 of pregnancy in 3M (n = 6), normal F3 (n= 6) and abnormal F3 (F3-A, n= 6) groups. (a) GzmB mRNA level. (b) NKP46 protein level. (c) End mRNA level. (d)

Eng mRNA level. (e) Vegf mRNA level. (f) Prl8a2 mRNA level. (g) Bmp2 mRNA level. (h) Hoxa10 mRNA level.
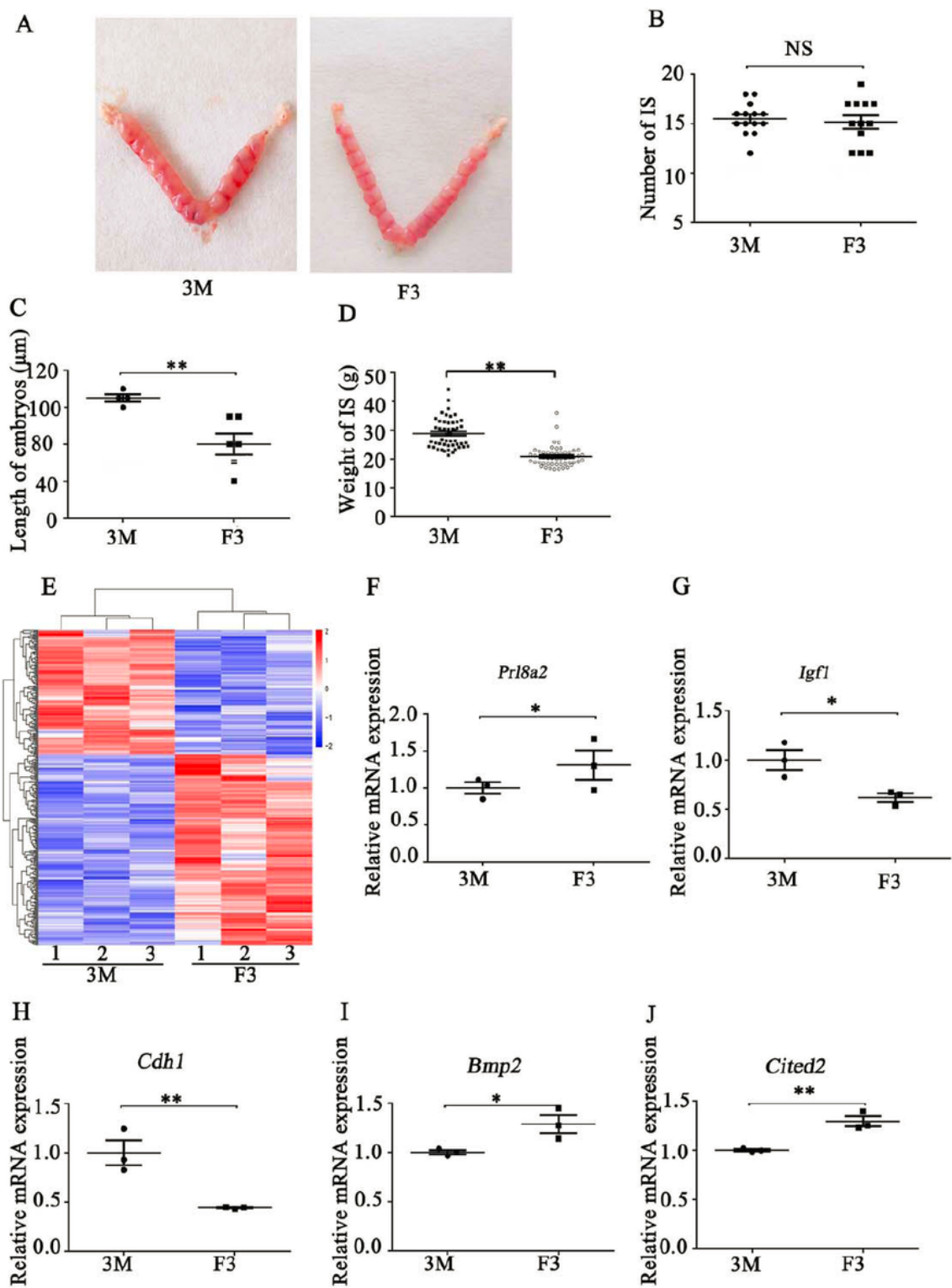
Figure 4

Decidual development on day 8 of pregnancy in F3 and 3M groups. (a) The uterine morphology on day 8 of pregnancy. (b) The average number of implantation sites in two groups. (c) The average length of embryo on day 8 in two groups. (d) The average weight of implantation sites on day 8 in two groups

(n=10). (e) Heatmap of genes differently expressed in the decidual tissues in two groups. (f) Prl8a2 mRNA level. (g) Igf 1 mRNA level. (h) Cdh1 mRNA level. (i) Bmp2 mRNA level. (j) Cited2 mRNA level.
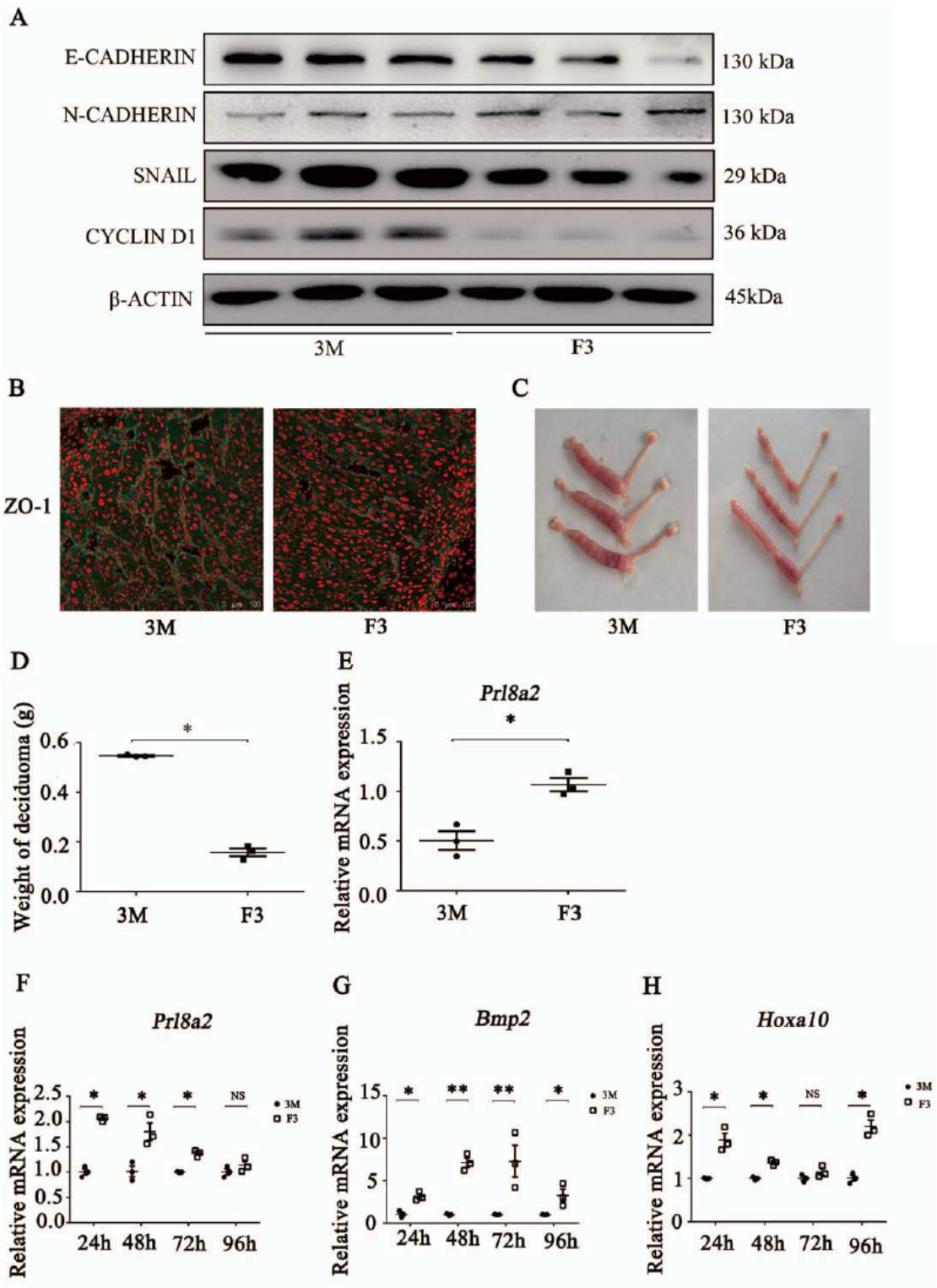
Figure 5

Decidualization-related gene expression in vivo on day 8 of pregnancy and in vitro. (a) The protein levels of mesenchymal−epithelial transition-related genes. (b) Immunofluorescence of Zo-1, an epithelial marker. Scale bars: 100 μm. (c) The morphology of deciduoma on day 8 of pseudopregnancy after 5μl

sesame oil were intraluminally injected in pseudopregnant mice. (d) The average weight of deciduoma in two groups. (e) Prl8a2 mRNA expression in two groups (n=6). (f) Prl8a2 mRNA level under in vitro decidualization. (g) Bmp2 mRNA level under in vitro decidualization. (h) Hoxa10 mRNA level mRNA level under in vitro decidualization.
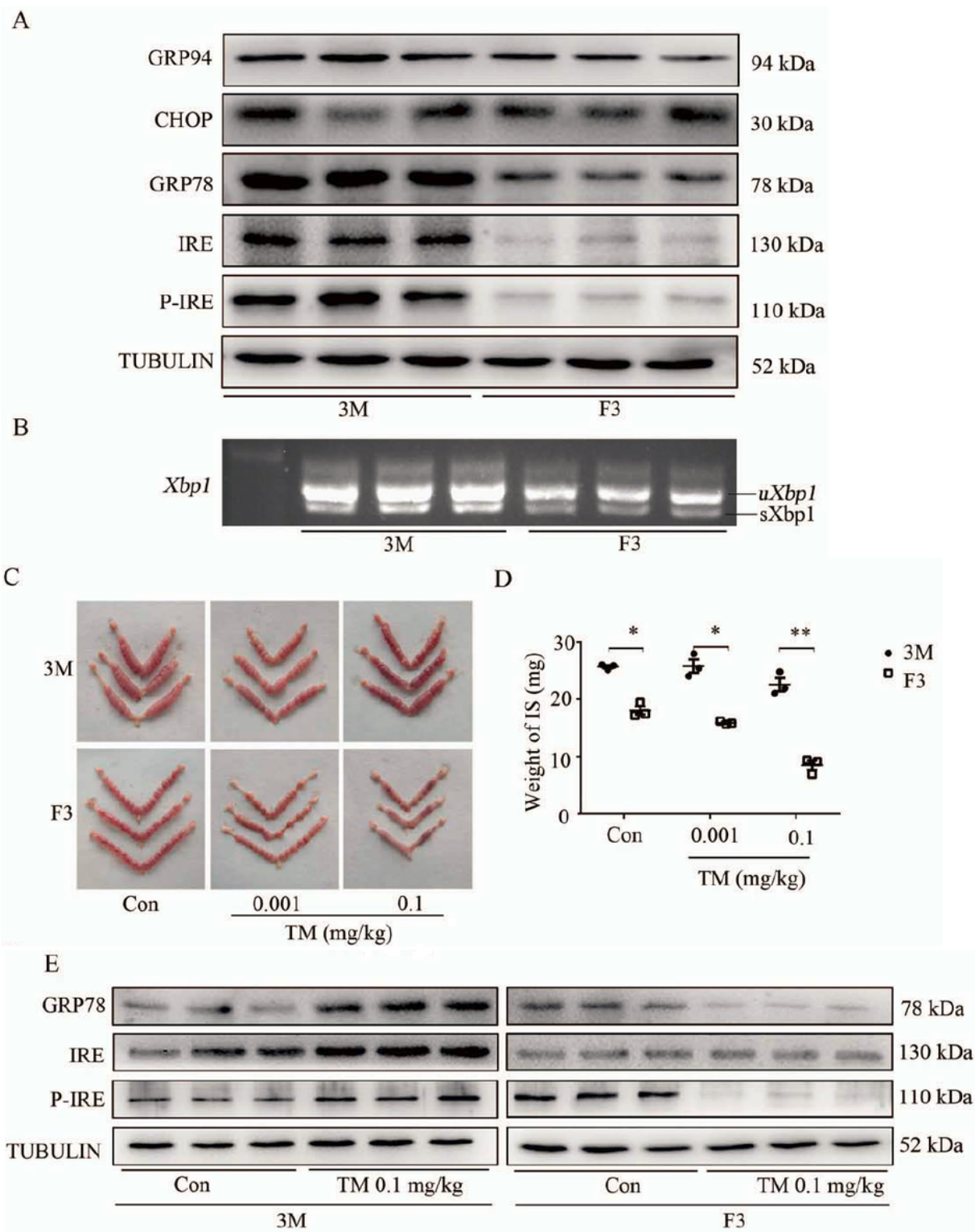

Figure 6

Endoplasmic reticulum stress in decidua on day 8 of pregnancy. (a) The protein levels of endoplasmic reticulum stress-related genes, including GRP94, CHOP, GRP78, IRE, and P-IRE in decidua on day 8 of pregnancy. (b) The relative level of XBP1, a downstream gene of GRP78-IRE pathway. (c) The morphology of deciduoma after pregnant mice were treated with 0.001 mg/kg and 0.1 mg/kg TM on days 6 and 7. (d) The average weight of implantation sites after pregnant mice were treated with 0.001 mg/kg and 0.1 mg/kg TM on days 6 and 7. (e) The protein levels of GRP78-IRE pathway-related genes at implantation sites on D8 after pregnant mice were treated with 0.001 mg/kg and 0.1 mg/kg TM on days 6 and 7 at 9:00 and 21:00, respectively.
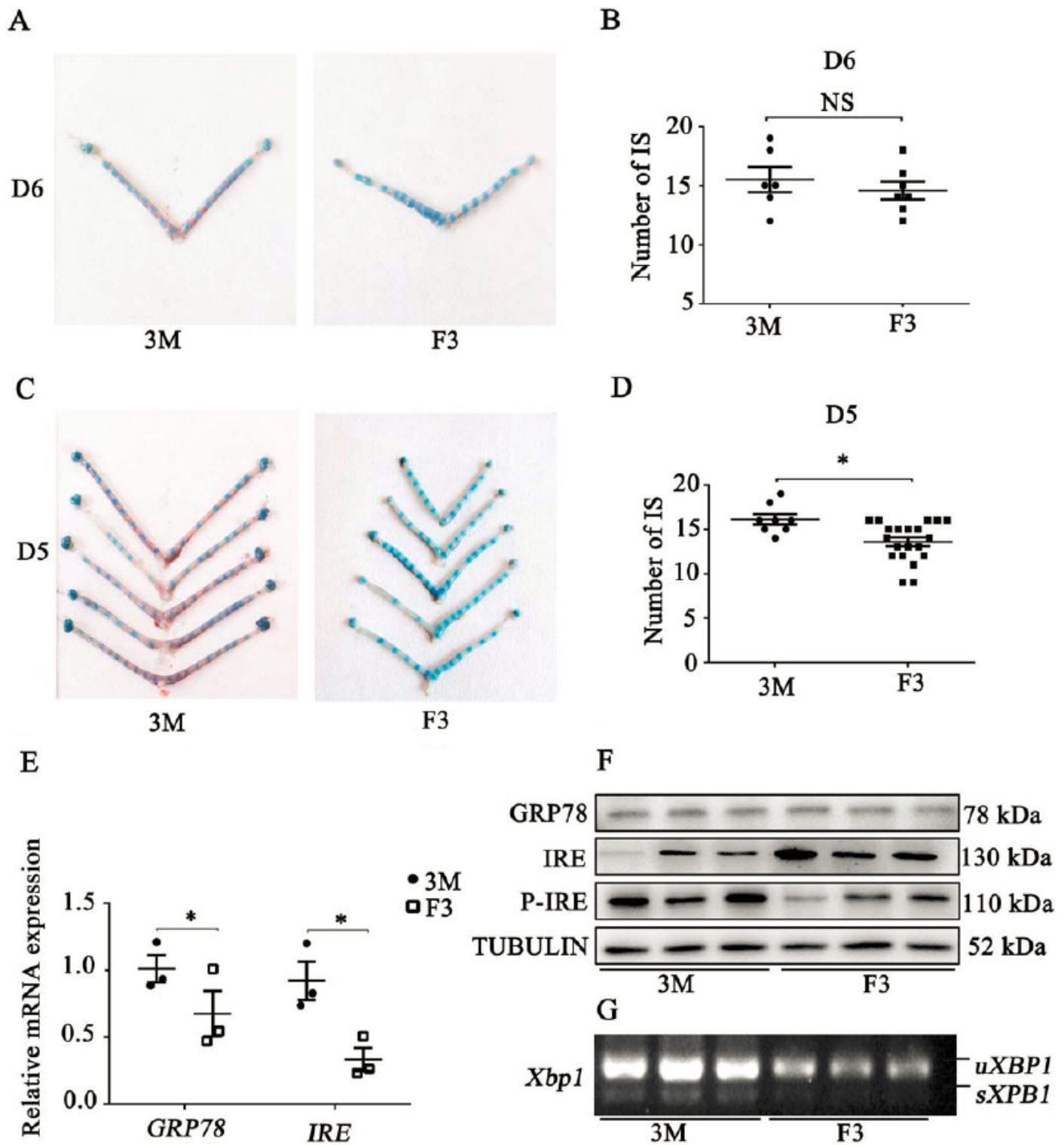
Figure 7

Embryo implantation and endoplasmic reticulum stress on days 5 and 6 of pregnancy. A The representative uterine morphology of implantation sites on day 6. (b) The average number of implantation sites on day 6. (c) The representative uterine morphology of implantation sites on day 5. (d) The average number of implantation sites on day 5. (e) The mRNA levels of Grp78 and Ire at implantation

sites on day 5. (f) The protein levels of GRP78, IRE and P-IRE at implantation sites on day 5. (g) The level of spliced Xbp1 at implantation sites on day 8.
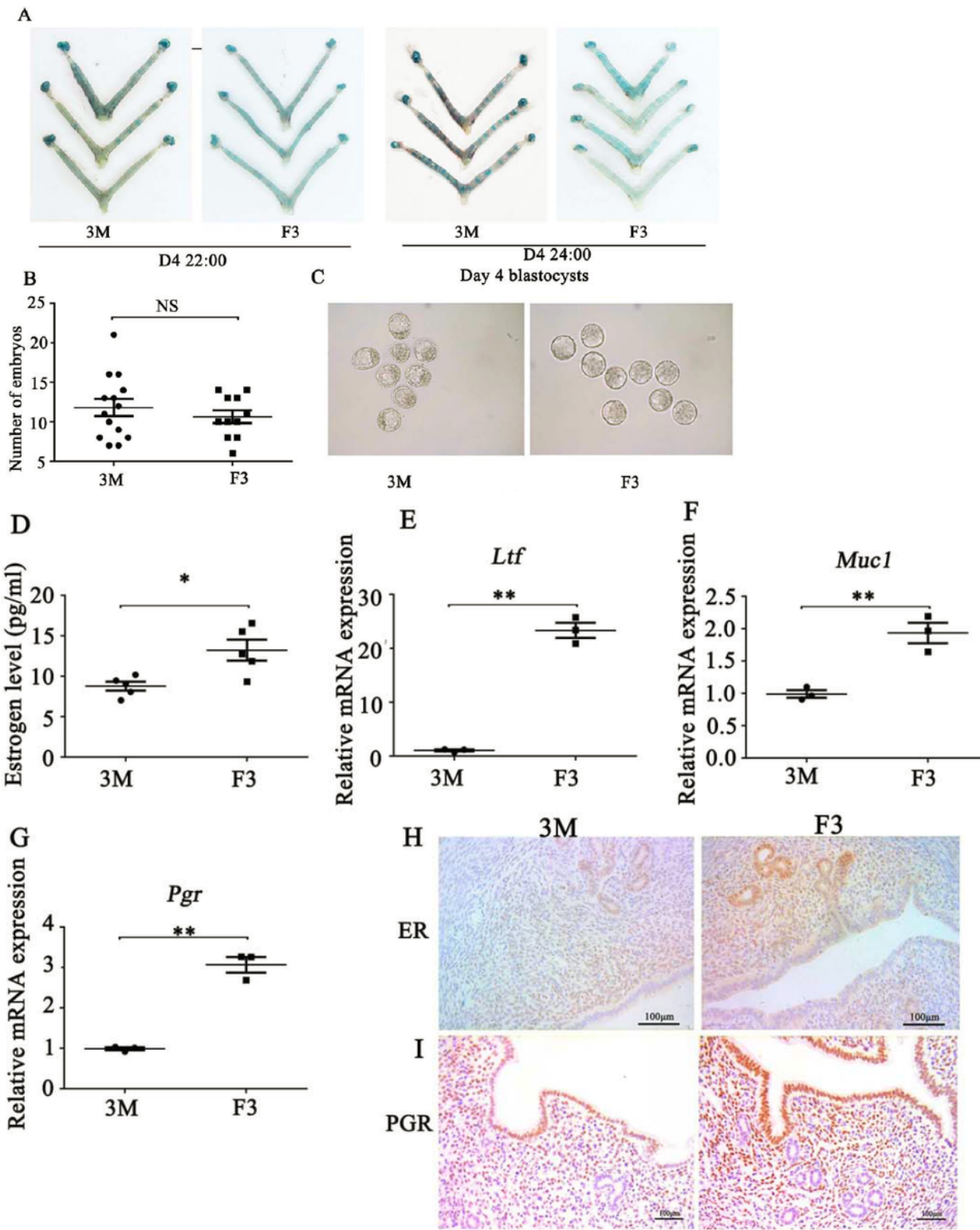

Figure 8

Embryo implantation and uterine receptivity. (a) The representative uterine morphology of implantation sites on day 4 at 22:00 and 24:00, respectively. (b) The average number of embryos collected from uterus at 09:00 on D4 (3M: n=14, F3: n=11). (c) The representative morphology of blastocysts collected from

day 4 pregnant mice at 09:00. (d) The serum level of estrogen on day 4. (e) The mRNA level of Ltf, an estrogen target gene. (f) The mRNA level of Muc1, an estrogen target gene. (g) The mRNA level of Pgr, an estrogen target gene. (h) Estrogen receptor (ER) immunostaining on day 4 of pregnancy. (i) Progesterone receptor (PR) immunostaining on day 4 of pregnancy.
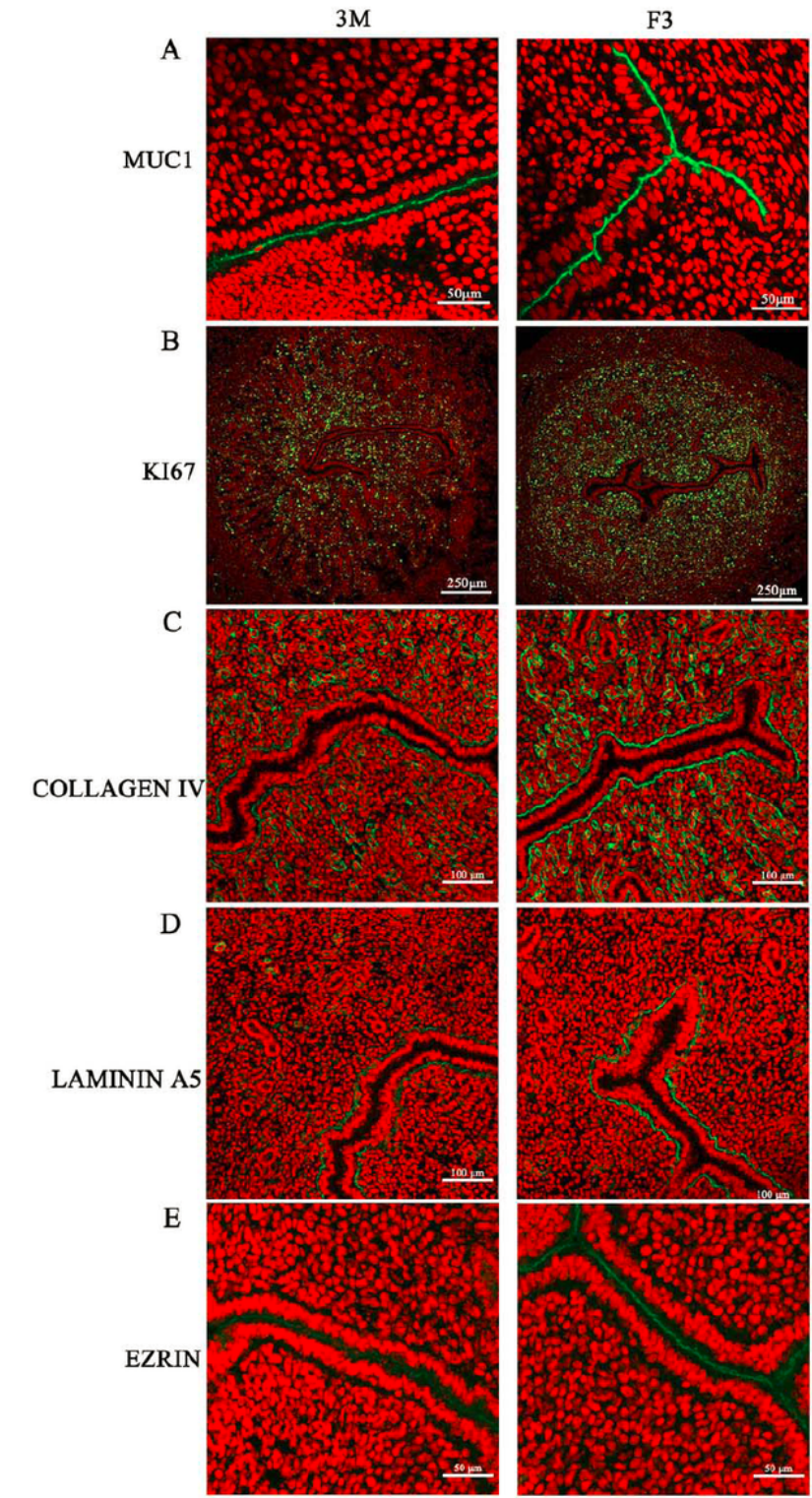

Figure 9

Immunofluorescence of uterine receptivity-related genes on day 4 of pregnancy. (a) MUC1. (b) KI67. (c) Collagen IV. (d) Laminin a5. (e) Ezrin.
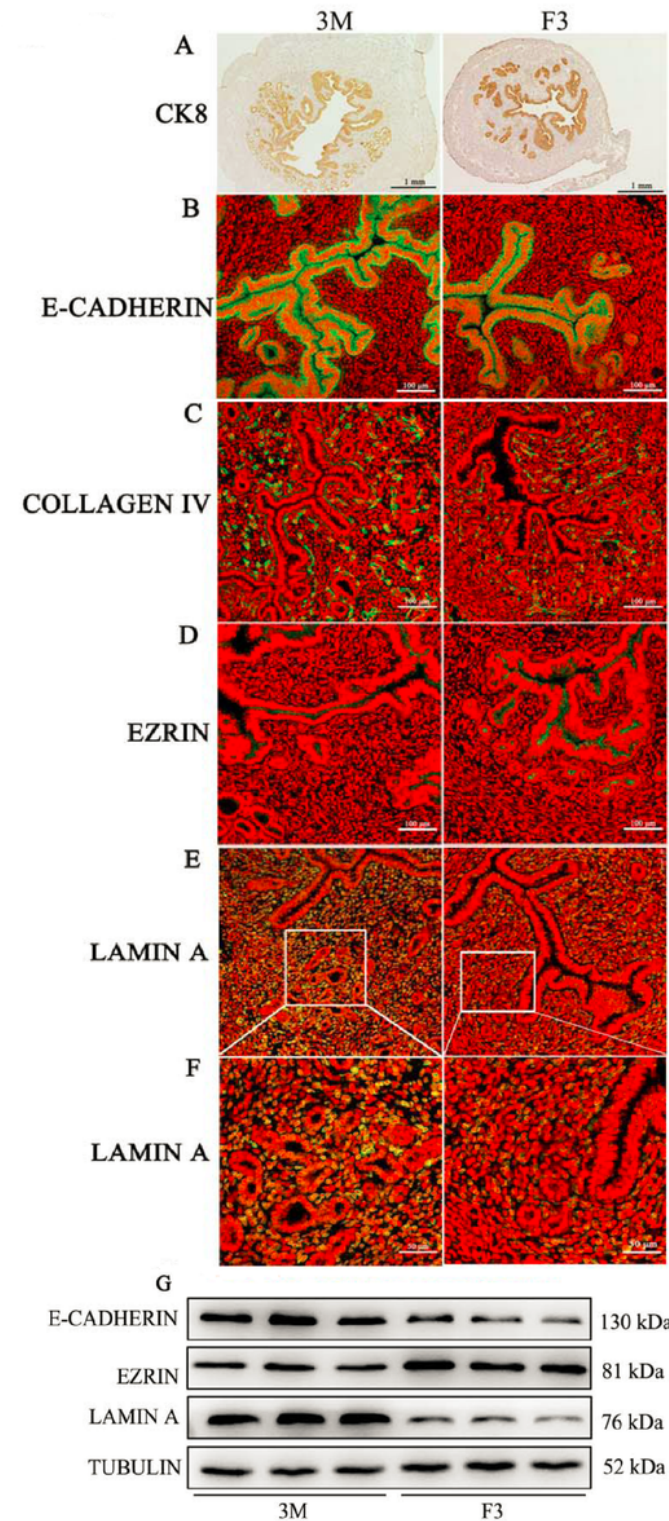

Figure 10

The morphology and gene expression of estrous uteri in 3M and F3 mice. (a) The uterine morphology immunostained with anti-cytokeratin 8 (CK8). (b) E-cadherin immunofluorescence. (c) Collagen IV

immunofluorescence. (d) Ezrin immunofluorescence. (E, F) LAMIN A immunofluorescence. (g) Western blot analysis of E-cadherin, Ezrin and Lamin A proteins.

Supplementary Files

This is a list of supplementary files associated with this preprint. Click to download.

- renamed5cfdd.docx